Simulation-based Study on the MAC Layer Performance of Cellular Vehicle to Everything (C-V2X) Communication

H K W Hettiarachchi

(169223M)

Thesis submitted in partial fulfillment of the requirements for the degree
Master of Science

Department of Electronic and Telecommunication Engineering

University of Moratuwa
Moratuwa, Sri Lanka

April 2022

Declaration

I declare that this is my own work and this thesis does not incorporate without acknowledgement any material previously submitted for a Degree or Diploma in any other University or institute of higher learning and to the best of my knowledge and belief it does not contain any material previously published or written by another person except where the acknowledgement is made in the text.

Also, I hereby grant to University of Moratuwa the non-exclusive right to reproduce and distribute my thesis, in whole or in part in print, electronic or other medium. I retain the right to use this content in whole or part in future works (such as articles or books).

Signature　　　　　　　　Date

The above candidate has carried out research for the Masters thesis under my supervision.

Signature of the supervisor　　　　　　　　Date

Abstract

Intelligent Transportation Systems (ITS) promise to deliver novel services related to various modes of transportation management, allowing users to have more coordinated and safer road trips. Cellular Vehicle to Everything (C-V2X) is a communication technology which can be integrated into ITS. It is introduced by 3GPP to be implemented as an LTE or 5G technology for the information transfer among vehicles or vehicles and other roadside infrastructure. Upon implementation of Mode 4 of C-V2X, the communication can be continued without the support of a base station. This study introduces the analysis of delay in C-V2X Mode 4 simulations on the popular simulator NS-3. It also has a comparison of delay and other parameters like Packet Reception Ratio (PRR) with results of a previous analytical model study. The simulation environment is built using available C-V2X related modifications of NS-3. An automation script is developed to run simulations efficiently for a range of different input scenarios of packet generation periods, node counts, Resource Reservation Intervals (RRIs), Resource Re-selection Probabilities (RRPs) and in random static User Equipment (UE) positions. The queuing behavior in transmitting packets is added newly to the simulator with both Cooperative Awareness Messages (CAM) and Decentralized Environmental Notification Messages (DENM) queues, hence the queuing delay is integrated with the results. The obtained PRR and delay variation comply with the analytical model. Furthermore, an analysis is done on the time difference between transmission and reception of a packet in the simulator, without adding the queuing delay, for comparison purposes.

Acknowledgement

This work was carried out during the years 2019-2021 at the Department of Electronic and Telecommunication Engineering, University of Moratuwa. I owe my deepest gratitude to my supervisor Dr.Tharaka Samarasinghe and Mr.Geeth Priyankara for their incredible guidance to successfully complete the research. I would like to thank all the authors and owners of the materials that have been referred to in this thesis and the authors of free online tutorials and other resources. Finally, I would like to express my gratitude to everyone who helped me accomplish the study, particularly my family members, fellow batch mates, and friends.

Contents

List of Figures

List of Tables

List of Abbreviations

P_{rk} Resource Keep Probability

3GPP 3^{rd} Generation Partnership Project

BSM Basic Safety Message

C-V2X Cellular Vehicle to Everything

CAM Cooperative Awareness Messages

CSMA/CA Carrier-Sense Multiple Access with Collision Avoidance

CSR Candidate Single-subframe Resource

D2D Device to Device

DENM Decentralized Environmental Notification Messages

DSRC Dedicated Short-Range Communications

ETSI European Telecommunications Standards Institute

IEEE Institute of Electrical and Electronics Engineers

ITS Intelligent Transportation System

LTE Long-Term Evolution

MAC Media Access Control

NIST National Institute of Standards and Technology

PHY Physical Layer

PIR Packet Inter-Reception

PRB Physical Resource Block

ProSe Proximity-based Services

PRR Packet Reception Ratio

PSCCH Physical Sidelink Control Channel

PSSCH Physical Sidelink Shared Channel

RB Resource Block

RC Re-selection Counter

RRC Radio Resource Control

RRI Resource Reservation Interval

RRP Resource Reselection Probability

RSRP Reference Signal Received Power

RSSI Received Signal Strength Indicator

SCI Sidelink Control Information

SPS Semi-Persistent Scheduling

SUMO Simulation of Urban MObility

TB Transport Block

TTI Transmission Time Interval

UE User Equipment

V2I vehicle-to-infrastructure

V2N vehicle-to-network

V2P vehicle-to-pedestrian

V2V vehicle-to-vehicle

V2X Vehicle to Everything

WAVE Wireless Access in Vehicular Environments

WINNER Wireless World Initiative New Radio

Chapter 1

Introduction

1.1 Motivation

Intelligent Transportation Systems (ITS) and automated vehicles are rapidly expanding multidisciplinary technology domains with a significant number of ongoing studies as well as a variety of new research requirements. This significance stems from their potential to reduce the road traffic congestion, minimize the number of road accidents, reduce the amount of energy consumed, minimize the time on the road and save human resources. Possible improvements and innovation plans for future ITS make an impact on the current automobile industry and other related fields like communication between automated or semi-automated vehicles. The development of autonomous or semi-autonomous driving technologies has increased the demand for the vehicle communication. To make it practical, communication must be virtually faultless in order to avoid harm to people and property. A very low latency range of a few milliseconds is also required for critical messages.

Vehicle to Everything (V2X) communication is basically the exchange of information between a vehicle and another entity through a wireless medium. V2X refers to vehicle-to-vehicle (V2V), vehicle-to-pedestrian (V2P), vehicle-to-infrastructure (V2I), and vehicle-to-network (V2N) communication. The V2X technologies are primarily being developed in two streams: C-V2X technology was introduced by the 3rd Generation Partnership Project (3GPP), while IEEE 802.11p was introduced by the Institute of Electrical and Electronics Engineers (IEEE).

This research is a simulation-based study on the performance of various C-V2X parameters and their implementation on the NS-3 simulator. As the benchmark, this entire study was based on two previous works: the C-V2X basic simulator code developed by Eckermann *et al.*[2] on NS-3, and the previous studies done by Wijesiri *et al.*[4][5]. In the simulator module, they have developed modifications for C-V2X on the Media Access Control (MAC), Physical Layer (PHY), Radio Resource Control (RRC) layers on basic NS-3 simulator and have done a study on some parameters except the delay. In the analytical model, they have built a discrete-time Markov chain and by solving it, they have generated results for the C-V2X parameters including delay. We note that the delay is a crucial performance metric in V2X communications. Hence, we extend the work in [2], by incorporating the delay elements associated with packet generation and packet queuing in the simulations. Moreover, the results are used to make a comparison with the results in [4] and [5], where the PHY layer parameters have been neglected.

1.2 Research Methodology

After the overall background literature study on C-V2X, the basic simulation is implemented as presented by Eckermann *et al.*[2] with the original conditions. A verification was done with comparing the code to the related 3GPP standards. The simulator was set up and studied using online resources. The simulation-based studies on C-V2X were found to be limited in the literature compared to IEEE 802.11p, which is a more mature technology.

There were 2 key objectives to achieve as planned initially. First to compare the result of basic NS-3 simulation with the results of analytical model by Wijesiri *et al.*[4]. Second, to setup a traffic situation like an intersection, traffic light, pedestrian crossing, ambulance maneuver, T junction, highway or a ramp on highway in the vehicular traffic simulation software SUMO and observe the behavior of MAC layer performance indicators such as delay, reception ratio and the reliability.

As mentioned above, the basic results were generated as benchmark simulation by Eckermann et.al [2]. However, when comparing with the analytical model [4], we observed some differences on basic interpretation. The delay was a significant parameter in the analytical model done using a discrete time Markov chain. However, in the simulator, the delay was almost neglected. Therefore, the delay was defined as a new modification in code. A queuing delay implementation on NS-3 is found in a queuing code developed for [5]. However, it is developed for WiFi based IEEE 802.11p, not C-V2X. With the help of it, the code in [2] is modified to add delay and also the other options like queuing. And the delay was calculated using the difference between the transmitting time and receiving time values recorded in logs.

In the initial stages of this study, we planned to integrate SUMO with NS-3 considering the behavior and response of physical mobility parameters like position and velocity. For that, we were able to integrate a mobility simulation done on SUMO with the NS-3 basic simulation developed for static random positions. However, due to the complexity on getting the results in an agreeable level compared with the analytical model even for a simple static positioning, the simulations were continued with the basic static mobility model before the addition of mobility.

The resource selection algorithm of C-V2X is the Semi-Persistent Scheduling (SPS). Understanding SPS and its implementation on NS-3 was considered as necessary. Finding resources on the NS-3 development on this particular technology was a challenge. Most of the research done on vehicular communication using NS-3 were focused on the WiFi based IEEE 802.11p standard, not C-V2X. As a result, a significant percentage of the time and effort invested on this study is dedicated to understanding NS-3 implementation and do the development on it.

When considering the delay, queuing delay is a key type. Since there was no queue in the basic simulator, packet queues were created as a modification as C++ object arrays. With the help of it, the total delay is calculated as a summation of both queuing delay and transmission delay. The propagation delay and processing delay can be easily neglected considering the type of this study.

The variation of input parameters was done using Python scripts. The developed scripts initiate various parallel NS-3 simulations in background which utilize the hardware resources of running computer optimally. Since some simulations take time up-to few hours, it was very important to make such automation for the execution of the simulator. The analysis of the result logs was also done using Python through the Jupyter Notebook environment.

1.3 Contributions and Outline of the Thesis

The main contribution of this study is the implementation of queuing and delay for C-V2X on NS-3 open source simulator. When running the simulator without modifications, it seems to give only the transmission latency, which is very small compared with the queuing delay. In this study, the queuing delay has been added and the effects of other parameters on the overall delay are observed. When considering the analytical model [4], it basically focused on the model of MAC layer. In this simulation-based platform, it enables to make analysis on the other layer effects as well.

After this introduction, background on C-V2X and other related studies are described in Chapter 2. It contains the necessary background information on the LTE frame structure related with C-V2X communication, the SPS algorithm, descriptions on parameters used in the study, and a literature review on currently available work in the literature. In Chapter 3, the simulation environment is described. It includes the building blocks of the simulation setup, integration method with mobility model and the list of simulations done. Chapter 4 describes the results obtained from the simulation and the comparison with the benchmark studies. Finally, Chapter 5 is added for conclusions and potential future work.

Chapter 2

Background and Related Works

2.1 C-V2X Elements and Standards

The 3rd Generation Partnership Project (3GPP) is a union of organizations interested in commercialized mobile and fixed cellular communication networks. The technologies commonly known as 3G, Long-Term Evolution (LTE), 4G and 5G are standardized by 3GPP. The initial and basic function of these 3GPP standards focused on the communication of regular wireless customers who connect to the base station with up-link and down-link. After the improved LTE standard numbered as Release 12, it has support for the direct communication over the side-link with technologies introduced as Proximity-based Services (ProSe) and Device to Device (D2D) communication [6]. ProSe direct communication allows two or more compatible user-equipment in the accessible range to create communication paths. For public safety specific usage, ProSe devices can make side links, and also, they are able to work as UE-to-Network relays with the participation of multiple devices [7].

Above direct communication enables User Equipment(UE) to communicate directly with each other, with or without the help of a base-station. They were introduced specially for public safety related applications. The ProSe specification defines PC5 interface, which is also used for C-V2X communication. Later, the Release 14 was introduced focusing Low-latency LTE. Since the vehicular communication needs lower latency in the range of few milliseconds, C-V2X is a highlighted technology with it.

There are four modes defined for LTE side link though only two modes are described in 5G [8]. In 3GPP Release 12, LTE Mode 1 and Mode 2 are described with a major emphasis on D2D services and other public safety applications. For V2X communication, Mode 3 and Mode 4 were introduced after Release 14 [9]. LTE Mode 3 side link is controlled by the infrastructure. But in Mode 4, it works independently even with no cellular network coverage. In this study, I have considered only LTE Mode 4 communication since it is the most critical implementation scenario.

2.1.1 Related Specifications

3GPP has introduced scenarios for how a vehicle can act with or without LTE network coverage in report TR 36.885 (Study on LTE-based V2X services) [10]. It describes the overall architecture including the core-network. It includes performance evaluation results for PRR, delay and power consumption. It also pays some attention to the coexistence with DSRC/IEEE 802.11p. Some realistic implementations are described in TR 22.885 (Study on LTE support for V2X services) [11] with pre-conditions, service flows, post-conditions and potential requirements.

All V2X applications (V2V,V2I,V2N,V2P) are described in TS 22.185 (Service requirements for V2X services) [12]. It also explains the basic infrastructure requirements for deploying a C-V2X system. After that, it describes the latency, reliability, message size and frequency, range, speed, and basic security needs for specific services.

The service requirements related with vehicles platooning, advanced driving, extended sensors, remote driving are specified in TS 22.186 (Enhancement of 3GPP support for V2X scenarios) [13]

The physical layer side-link (PSSCH and PSCCH channels) behavior with four modes of V2X transmissions is described in extensive detail in Chapter 14 of the TS 36.213 (E-UTRA Physical layer procedures) [9]. MAC layer of the side link is thoroughly discussed in chapter 5.14 of TS 36.321 (E-UTRA MAC protocol specification) [14]. In TS 36.331 (E-UTRA RRC Protocol specification) the sidelink related RRC specifications are described in chapter 5.10 [15].

Most of the C-V2X related 3GPP specifications and reports are summarized in Table 2.1. Some specifications on the core network architecture and security aspects are not in the scope of this study.

Another prominent institution dealing with telecommunications, television, and other electronic communications networks and services is the European Telecommunications Standards Institute (ETSI). In addition to 3GPP, ETSI also publish their own specifications. ETSI TS 103.613 (Access layer specification for Intelligent Transportation System using LTE Vehicle to Everything communication in the 5,9 GHz frequency band) [16] describes related spectrum in 5.9 GHz band, defines the values for parameters of C-V2X, and concludes other related ETSI specification documents. CAM and DENM message definitions, function and generation scenarios are described in ETSI EN 102 637-2 [17] and ETSI EN 102 637-3 [18]

Number	**Topic**	**Relevant Information**
TS 23.303	Proximity-based services (ProSe) [7]	ProSe architecture and functions
TR 36.885	Study on LTE-based V2X services [10]	V2X operation scenarios Technical support Architecture (core network) Evaluation results
TR 22.885	Study on LTE support for V2X services [11]	Use cases Potential requirements
TS 22.185	Service requirements for V2X services [12]	V2X applications Application requirements
TS 36.101	UE radio transmission and reception [19]	Spectrum allocation
TS 36.211	Physical channels and modulation [20]	Slot structure and physical resources(in chapter 9)
TS 37.985	Overall description of RAN aspects for V2X based on LTE and NR [21]	Side link resource allocation structure Physical channels and band information 4G and 5G side link modes
TR 36.785	V2V services based on LTE sidelink; UE radio transmission and reception [22]	Frequency ranges, Bandwidths Simulation assumptions Sample parameter values Simulation results
TS 22.186	Enhancement of 3GPP support for V2X scenarios [13]	V2X with special automated vehicle services
TS 36.213	E-UTRA Physical layer procedures [9]	UE procedures related to side-link (chapter 14)
TS 36.321	E-UTRA MAC protocol specification [14]	MAC layer of the Sidelink (chapter 5.14)
TS 36.331	E-UTRA RRC Protocol specification [15]	side-link related RRC specifications (chapter 5.10)
TS 23.285	Architecture enhancements for V2X services [23]	V2X related architecture and functions in core network
TS 23.286	Application layer support for V2X services; Functional architecture and information flows [24]	High level core deployment architectures Data flows
TR 23.785	Study on architecture enhancements for LTE support of V2X services [25]	Potential architecture enhancements
TS 23.287	Architecture enhancements for 5GS to support V2X service [8]	V2X deployment and changes on 5G

Table 2.1: Related 3GPP documents

2.1.2 Spectrum Allocation and Resource Structure

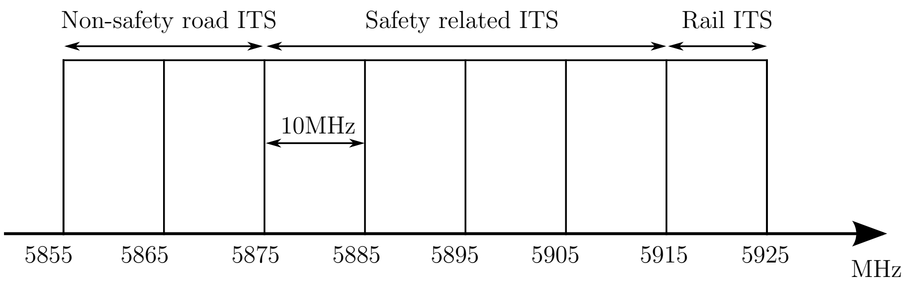

Figure 2.1: Spectrum designations at 5.9 GHz in Europe [1]

The spectrum allocated for ITS is not the same for every region or country. However, most of them use the frequency band around 5.9GHz. For the C-V2X side link(PC5 interface), 3GPP defined band 47 (5855-5925 MHz) is allocated [19]. For vehicle-to-network (V2N) communication (Uu interface), normal LTE mobile frequency bands are used.

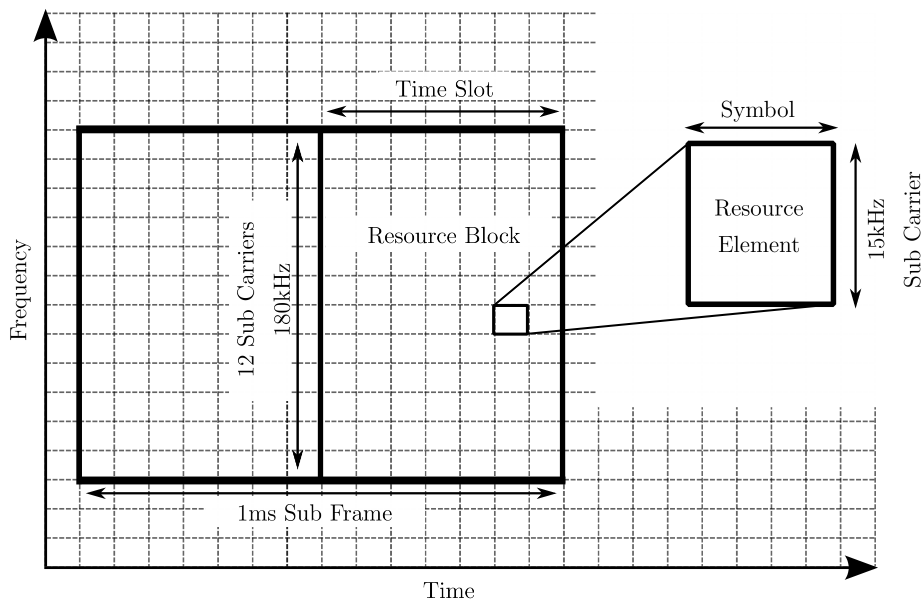

Figure 2.2: Resource Definitions

The smallest unit of LTE resource frame structure is the Resource Element having 15kHz bandwidth in frequency domain and one symbol duration in time domain. There are 6 or 7 symbols(This count depends on whether the cyclic prefix is Normal or Extended type) for time slot and two time slots take 1 millisecond time which is called a sub frame [20]. A Physical Resource Block (PRB) is defined as containing frequency-time resources such as having 12 contiguous resource elements(=180kHz band width) within one time slot. As an example, in frequency domain, there are 50 PRBs in 10MHz (10MHz = 180kHz $\times$ 50 + 1MHz guard band).

Structure of the resource pool is described in [21]. A sub channel is defined as non-overlapping sets of PRBs within a sub frame with more than 3 PRBs. Resource allocation, sensing, and resource selection are done in sub channel units though some of the PRBs within a sub channel might not be utilized.

2.1.3 Channels and Modulation

The information transferred through the side-link has two major components.

1. Transport Blocks (TBs) with the data packet; Transmitted through Physical Sidelink Shared Channel (PSSCH)

2. Sidelink Control Information (SCI) with control information needed to maintain the connectivity; Transmitted through Physical Sidelink Control Channel (PSCCH)

For the arrangement of PSSCH and PSCCH in the resource pool, there are two scenarios called adjacent and non-adjacent. In adjacent scenario, it assigns an edge pair of PRBs of the sub channel to PSCCH. The rest of the PRBs of sub channel are employed to transmit PSSCH. In the Non-adjacent scenario, PRBs at the lowest frequencies of the resource grid are allocated for PSCCH as pairs of PRBs for all transmissions and upper part is dedicated for PSSCH sub channels separately.

PSSCH uses QPSK, 16QAM or 64QAM as modulation schemes according to the available channel conditions. PSCCH always uses QPSK [20] [26]. The LTE-V2X side link physical channels uses SC-FDMA as the multiple access scheme [21].

2.1.4 Propagation Model

A single ubiquitous radio access system is developed by the project Wireless World Initiative New Radio (WINNER) which is adaptable to a comprehensive range of mobile communication scenarios from short range to wide area [27]. For the V2V analysis, 3GPP TR 36.885 [10] used WINNER+ B1 path loss model which is a further development of WINNER II models. The base simulator of this study [2] used the same model programmed in the code. An analysis of the channel model is found in [28].

The WINNER+ B1 channel model is also known as UMi(Urban microcell scenario). As defined in [3], the equations for the channel model are described in Table 2.2.

	Path loss [dB]	Applicability range and antenna height default values
Line of Sight (LOS)	$PL = 22.7\,log_{10}(d_1) + 41.0 + 20\,log_{10}\left(\frac{f_c}{5.0}\right)$ $PL = 40.0\,log_{10}(d_1) + 9.45 - 17.3\,log_{10}(h'_{BS}) - 17.3\,log_{10}(h'_{MS}) + 2.7\,log_{10}\left(\frac{f_c}{5.0}\right)$	$10\,m < d_1 < d'_{BP}$ $d'_{BP} < d_1 < 5$ km $h_{BS} = 10m$, $h_{MS} = 1.5m$ $h'_{MS} = h_{MS}$-1 $h'_{BS} = h_{BS}$-1 $d'_{BP} = 4 \cdot h'_{BS} \cdot h'_{MS} \cdot \frac{f_c}{c}$ $c = 3 \cdot 10^8$ m/s
Non Line of Sight (NLOS)	$PL = \min(PL(d_1, d_2), PL(d_2, d_1))$ Where $PL(d_k, d_l) = PL_{LOS}(d_k) + 20 - 12.5n_j - 10n_j log_{10}(d_1) + 3\,log_{10}\left(\frac{f_c}{5.0}\right)$ And $n_j = \max(2.8 - 0.0024d_k, 1.84)$ PL_{LOS} is the path loss of B1 LOS scenario and $k, l \in \{1,2\}$	10 m $< d_1 < 5$km, $\frac{w}{2} < d_2 < 2$km $w = 20$m (Street width) $h_{BS} = 10$m , $h_{MS} = 1.5$m When $0 < d_2 < \frac{w}{2}$ the LOS PL is applied

Table 2.2: WINNER+ B1 model [3]

2.2 Related Parameters and Performance Metrics

To measure the performance of C-V2X communication, there are several parameters we can change and performance metrics we can observe.

2.2.1 Basic Parameters

The key related parameters are:

1. Position
2. Velocity
3. Node Count
4. CAM packet rate
5. Resource reservation interval / T_1 and T_2/ Γ
6. Resource re-selection probability / resource keep probability
7. Modulation and coding scheme (MCS)

Resource Reservation Interval (RRI), Selection Window Size(Γ) and T_1,T_2 Values

These three types of parameters are related to each other and widely used in various publications. The T_1 and T_2 values are simply the time values (milliseconds) of start and end sub-frames of the selection window. This time is measured from the T(resource re-selection) time as illustrated in Figure 2.3. According to the standard, these values have to satisfy the constrains $T_1 \leq 4$ms and $20\text{ms} \leq T_2 \leq 100$ms. In the simulator T_1 and T_2 values are directly defined, and the user is able to set them.

In the simulator [2], the Resource Reservation Interval (RRI) value is defined separately as the resource reservation period. It is set to the value of 100ms in basic simulations, but they have changed it and observed the effect of it. As mentioned in [26], vehicles use RRI included in the SCI to inform when they utilize the reserved sub-channel, and the value of it may take 20ms, 50ms, 100ms or any multiple of 100ms.

Within the LTE frame structure, a UE will get a sub-frame to do the transmission in a particular group of Resource Blocks (RBs). It will have one opportunity in only one sub-frame for a selection window. When the number of UEs increased, the selection window size has to be increased to give chances as much as possible. The selection window size is related with latency, because after one transmission, a UE has to wait until the next selection window.

In the analytical model [4][5], the selection window size is denoted by Γ. This value could be 100ms, 50ms, or 20ms. When considering about this name and the usage, it has to be the difference between above T_1 and T_2 values. However, when comparing the results, it is more similar to the RRI.

Resource Re-selection Probability / Resource Keep Probability

In Semi-Persistent Scheduling (SPS), the probability to keep the selected resource without doing re-selection is called the Resource Keep Probability (P_{rk}). According to the standard, this P_{rk} can be configured within the range [0,0.8]. The Resource re-selection probability is the probability to make a new selection of the next transmitting resource. Therefore, it has the value $1 - P_{rk}$, which is in the range [0.2,1].

2.2.2 Performance Metrics

The key related performance metrics we can observe are:

1. Delay (Transmission,Queuing,Propagation,Processing)

2. Packet reception ratio / Collision probability / Queuing loss

3. Packet Inter Reception (time between two successful receptions of two different successive packets transmitted from node A to node B)

4. Channel Utilization

5. Throughput

Delay

There are four types of delay:

1. Transmission delay
   The time period needed to push the packet's data bits into the transmission medium is known as transmission delay. This value depends on the size of the packet and the band width. It does not depend on the distance of the medium. The LTE Transmission Time Interval (TTI) (1ms) is a significant contributor to the transmission delay in our case.

2. Propagation delay
   The time of one particular bit to go through the distance of propagation medium is defined as propagation delay. Since we consider the wireless medium here, propagation delay is the ratio (distance between TX and RX)/(speed of light), assuming the speed of radio waves in air medium is closer to speed of light. We consider distances in few hundred meters for C-V2X side link, the maximum of this delay is in the range of 1 or 2 μs. Since we know that when there is the compulsory transmission delay value in range of 1000 μs, we can simply neglect this propagation delay.

3. Queuing delay
   The time between a packet being queued and it being sent is defined as the queuing delay. This value depends on the amount of traffic and the queuing algorithms. C-V2X transmissions may have queuing delays up to 100ms.

4. Processing delay
   The time period spent by network devices to check the packet header and determine where the packet must be sent is defined as processing delay. This value depends on the routing table, execution of the data structures of the system and hardware implementation nature. The processing delay occurs in higher layers of network stack. This value is not considered in this research since we only consider the direct device to device transmissions through radio interface in access network.

The measured end to end delay is usually the sum of all four delay values. In our case, it is the sum of the transmission delay and the queuing delay. In C-V2X analysis, the knowledge about delay is very important because it may make life and property damages if a critical message is not received within the required time period.

Packet Reception Ratio (PRR)

The Packet Reception Ratio is calculated by X/Y , where Y is the number of nodes that are located in the baseline distance from the transmitter, and X is the number of nodes with successful packet reception among Y [2].

Packet Inter-Reception Time (PIR)

Packet Inter-Reception(PIR) is the time between two successful receptions of two different successive packets transmitted from node A to node B [2].

Throughput

Throughput of a system is the number of units of data it can handle in a given length of time. For one resource element, data capacity is 2bits for QPSK, 4bits for 16QAM and 6bits for 64QAM. If we get the number of symbols per slot as 7, for a PRB there are 84 resource elements (7×12 sub carriers). As an example, when we consider the modulation scheme as 64QAM, there are 84×6 bits in an RB. For 1ms sub-frame and 10MHz channel, the maximum capacity is $84 \times 6 \times 2 \times 50 = 50400$ bits. To get the throughput, we have to measure how much of this maximum capacity is utilized by a particular UE.

2.3 Semi-Persistent Scheduling (SPS)

The resource selection of radio access equipment for LTE side-link Mode 4 is done using sensing-based Semi-Persistent Scheduling (SPS) algorithm. SPS is used in other LTE applications also and described in 3GPP standards and various related studies [9] [14] [26] [4]. Equipment in the vehicle estimates available resources by sensing the previous transmissions of all neighboring vehicles. After that, it can select an optimum radio resource for next transmission.

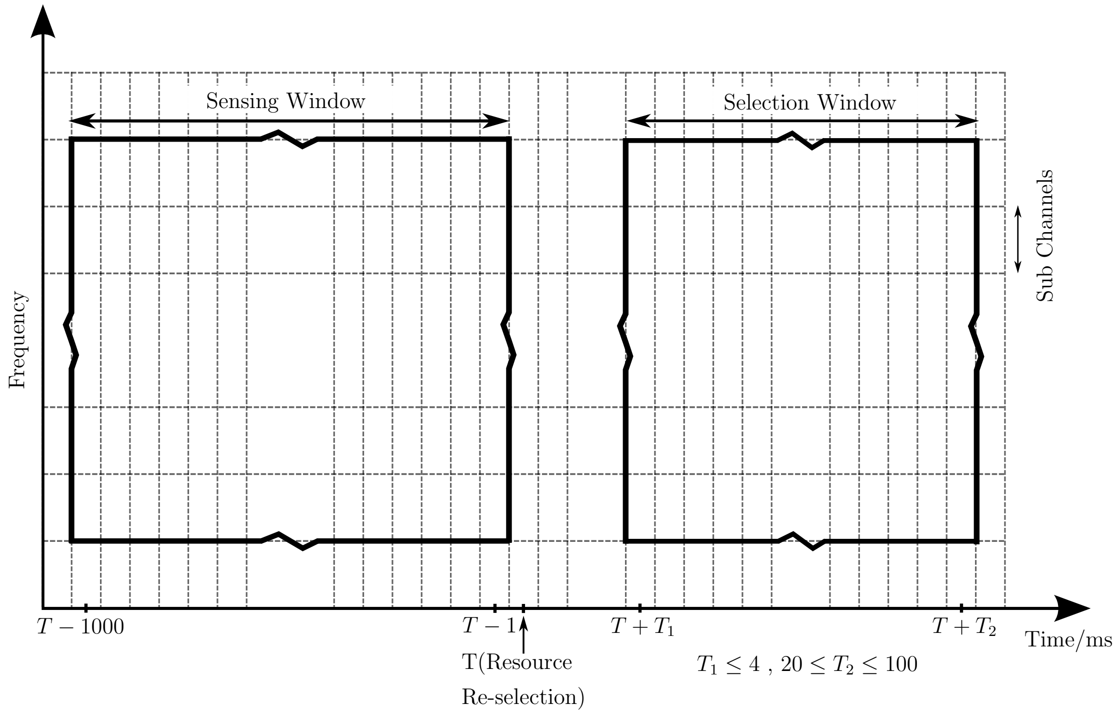

Figure 2.3: Semi-Persistent Scheduling

Candidate Single-subframe Resource (CSR)

A group of adjacent sub channels within the same sub frame where the new Sidelink Control Information (SCI) + Transport Block (TB) to be transmitted fits.

Selection Window and Sensing Window

The selection window is the time period which the vehicle has to select a CSR for the transmission. It is defined when the resource re-selection or the packet generation is done. Length of the selection window is the latency deadline of the generated packet [21]. If the re-selection time instance is T, the start instance of selection window is $T + T_1$ and end of the selection window is $T + T_2$ where $T_1 \leq$ 4ms and 20ms $\leq T_2 \leq$ 100ms.

Sensing window is the time period containing the last 1000 sub-frames before the re-selection time T, as illustrated in Figure 2.3. The vehicle considers all received transmissions from other vehicles during the sensing window.

Re-selection Counter (RC)

RC is a value which is used for the selection of resources. It decrements by 1 after each transmission. An initial value for it, is randomly selected with equal probability from ranges:

1. [5,15] for RRI>=100ms

2. [10,30] for RRI=50ms

3. [25,75] for RRI=20ms

Sub-channel Selection

A new sub channel is selected if at least one of following conditions is satisfied:

1. If RC reaches 0, with a probability 1-P_{rk}. This P_{rk} is the probability of resource keep which is configured in range [0,0.8]. Therefore, the 1-P_{rk} value is in range [0.2,1] is known as the resource re-selection probability. When RC reaches 0, if the vehicle does not keep the same sub channel again, it will indicate that to other nodes by changing RRI value in SCI to 0.

2. The higher layers might transfer packets with various lengths. If the size of next packet to be transmitted is higher than the reserved resources size, the device has to select a new resource.

3. If the current reserved sub channel(s) cannot satisfy the latency requirements, then also the device has to select a new resource.

If the device decides to select a new resources for transmission, it will follow three steps:

1. Identify the possible CSRs in the selection window.

2. The C-V2X equipment in the vehicle can exclude CSRs from above selected set with the highest interference from other peer vehicles' transmissions. For that, it uses the information collected in the sensing window.
   A CSR is excluded if:

   (a) The considering vehicle has taken the correspondent CSR during the sensing window. Because of the half duplex nature, sensing is not performed when transmitting.

   (b) Received an SCI from another vehicle indicating it will utilize the CSR.

   (c) The correspondent CSR in the sensing window has average Reference Signal Received Power (RSRP) higher than the configured threshold.

   If the list of not excluded CSRs is denoted by L_1, and if L_1 has less than 20% of all CSRs, then increase the above threshold by 3dB and this step has to be iterated again.

3. Create the list of CSRs L_2 from L_1, such as having the lowest average Received Signal Strength Indicator (RSSI) values. This averaging is done for previous 10 sub-frames [4]. The number of CSRs in L_2 is limited to 20% of all CSRs in the selection window.

Then it will select a random CSR from L_2 for the next number of transmissions decided with Re-selection Counter.

2.4 C-V2X Packet Types

Cooperative Awareness Messages (CAM) and Decentralized Environmental Notification Messages (DENM) specified by ETSI are the prominent message types used for C-V2X communication. They are described in ETSI EN 102 637-2 [17] and ETSI EN 102 637-3 [18] specifications. Basic Safety Message (BSM) is another message type previously introduced with DSRC. The BSM behaves similarly to CAM, and 3GPP specifications support them as well [21]. In this study, we implement only the CAM and DENM packets.

The CAM messages are usually transmitted with similar intervals of time with regular information like heading, position(longitude,latitude) and speed. The generation interval is in between 100ms to 1000ms. The CAM message size is within 121 to 320 Bytes without certificate and about 230 to 429 Bytes with certificate [10]. However, for evaluation purposes, they were modeled as periodically occurring sets of one 300-byte message followed by four 190-byte messages.

The DENM messages are transmitted with information of special events which will occur randomly. If a man or animal interruption of the motion(sudden brake) or the vehicle decided to change the lane, a DENM will be generated. Because of the nature of DENMs, they can be modeled as a random process with Poisson distribution of time periods between messages. Because of the criticality of DENMs, it needs to be received by peers with more reliability. Therefore, after the first transmission, the DENM is repeated for limited number of times with equal time intervals. In [29], they have done an analysis about these DENM messages and the improvement of reliability using repetitions. A DENM generation process has three main attributes when we model its behavior. They are the λ value (1/mean) of the Poisson distribution of DENM generation periods, number of repetitions per each packet(K), and the repetition interval(T_D).

2.5 Other Related Technologies

The family of standards 802.11 developed by Institute of Electrical and Electronics Engineers (IEEE) is focused on wireless local area networking, which is generally known as Wi-Fi. IEEE 802.11p is a standard in that group specifically developed for vehicular communication. It uses Carrier-Sense Multiple Access with Collision Avoidance (CSMA/CA) as the MAC layer protocol while C-V2X uses SPS. Wireless Access in Vehicular Environments (WAVE) is a mode of operation used by IEEE 802.11p device in order to operate in the Dedicated

Short-Range Communications (DSRC) band centered at 5.9GHz. ITS-G5 is a IEEE802.11p and ANSI/IEEE Std 802.2 based technology definition set standardized by ETSI (European Telecommunications Standards Institute)[2]

There are number of studies done on the performance comparison between these two technologies. Nevertheless, on the implementation of V2X communications practically, 3GPP technologies have more feasibility because it has well organized infrastructure already spread on a large geographical area. Therefore, if a country need to deploy the V2X infrastructure, it will be more cost effective for C-V2X than IEEE 802.11p based technologies[30]. Also, the 3GPP communications are mostly maintained by large telecommunication service providers in a country like Sri Lanka and therefore, it will be a boost to the implementation of C-V2X when consider the commercial advantage.

2.6 Related Studies

Several studies have already been done suggesting various optimizations and adjustments because vehicular communications is an emerging topic. Small packets are used in the V2X communication while the application's criticality necessitates high reliability and low latency. Some studies used simulations to verify the results, while some of them concluded the results obtained by analytical approaches. Furthermore, some studies have been validated utilizing empirical data obtained through physically implemented apparatus.

For D2D communication, a simulation-based study is done in [31] using the NS-3 as the simulation environment. It has the basic D2D communication implementation, which is the preliminary stage of C-V2X communication. Another simulation study is done in [32] to observe the impact of transmission power under varying density of vehicles for C-V2X Mode 4.

The simulator developed by Eckermann *et al.*[2] is the initial simulation platform for this study. They have implemented the C-V2X Mode 4(LTE Rel.14) related needs on a previous code by National Institute of Standards and Technology (NIST) created for D2D communication [31] on NS-3 release 3.28. They use WINNER+ B1 as the channel model. In the developed simulator for C-V2X, two scenarios have been simulated using SUMO as the mobility:

1. Static worst-case scenario (250 vehicles in 100m x 100m intersection)
2. 3GPP Manhattan grid

Nabil *et al.*[33] have done a performance analysis with introducing a C-V2X Mode 4 simulator based on NS-3. It has been done before the environment introduced by Eckermann *et al.*[2] and suggests that the RRI significantly influences to the data rate performance while RRP has a little effect.

Molina-Masegosa *et al.*[34] have evaluated the LTE V2V performance of Mode 4 and operation in urban scenarios with realistic traffic conditions. They have implemented the simulation using the Veins platform which integrates OMNET++ for wireless networking simulation and SUMO for vehicular traffic. In their results, the main considerations are packet delivery rate with the changes of Tx-Rx distance. In [35], they have implemented another simulation to determine optimum configuration for Mode 4. Same research group has done [26] on the comparison between IEEE 802.11p and C-V2X using the same simulation platform.

Jeon *et al.*[36] have done a study on SPS with their own developed simulator using Python. In this study, they have focused on avoiding message collisions, suggesting some modifications on the standard. Another simulation-based study is done by Wang *et al.*[37]. It uses a mobility model of a highway scenario as a system-level simulation. A performance analysis is done in [38] using a high-fidelity simulator based on NS-3 for an environment with the vehicles in highly congested network.

A Matlab based simulation study for the physical layer of all V2X technologies is done in [39]. In [40], ITS technologies ITS-G5 and C-V2X are compared by evaluating the performance of both physical layer and MAC layer. A study on the reliability of V2V communication is done in [41] assuming orthogonal street systems.

For an industrial park scenario, a study is done on the performance of a C-V2X network in [42]. They have evaluated the line-of-sight and non line-of-sight performance for each type of C-V2X communication. [43] proposes Non-Orthogonal Multiple Access (NOMA) concept for C-V2X Mode 4. A comparison of the performance of C-V2X and DSRC is done in [44] for the link level and system level. They conclude that C-V2X has ability to save more lives than DSRC in the road. Another comparison and analysis are included in [45]. They describe the performance of V2V communications, which is measured in terms of latency and reliability. Furthermore, an analysis with highway platooning is also taken in. [46] [47] and [48] are also performance comparison studies. [49] has described their prototype that has been developed to validate both CAM and DENM messaging capabilities. In [50], they evaluate the performance of different connectivity alternatives based on LTE-Advanced. A new short-term sensing-based resource selection method is introduced in [51].

Wijesiri *et al.*[4] have developed analytical models for both IEEE 802.11p and C-V2X Mode 4 to do a comparison of the performance of MAC layer parameters. They developed expressions for key performance metrics (average delay, collision probability, and channel utilization) using multi-dimensional Discrete-Time Markov Chain (DTMC) models coupled with DTMC based queuing models and traffic generators for both CAM and DENM packets.

Some numerical results also calculated for a highway scenario. They reveal that IEEE 802.11p outperforms C-V2X Mode 4 in terms of average delay. However, when it comes to collision resolution, C-V2X Mode 4 excels. As a benchmark for MAC layer parameters, we have used the results of this analytical model.

With the comprehension of all above resources of this literature survey, any simulation-based study done on NS-3 has not studied the delay of packets. Therefore, we can conclude that, there is a knowledge gap on doing simulated analysis on the packet delay of C-V2X using the NS-3 powerful simulator, which can be developed further for the advancement of this field.

Chapter 3

Simulation Environment

3.1 Simulator Setup

3.1.1 The Simulator

The NS-3 program is a discrete-event network simulator designed primarily for educational and research purposes [52]. It is a free, open-source software project that is maintained by a global community under the GNU GPLv2 license. When comparing with the popular simulator OMNET++, NS-3 does not depend on a GUI to build its simulations. Therefore, NS-3 can be expected as a friendly environment for automation than other simulators. In this research, above nature of NS-3 is widely used to do simulations for various variable values by automating it using Python scripts.

The NS-3 simulator is basically written in C++ language. However, it has some extensions using Python. The users can alter and enhance NS-3. They can utilize the given example scripts in this simulator. However, it is expected that the majority of users wish to develop new scripts, change or add to the simulator models according to their requirements. In this case, we use the code build around LTE helper library.

The initial setup is done with the support of tutorials in the official website [52] and the repository published by the contributors of C-V2X support on the simulator [2]. As the platform, a personal computer is used with Ubuntu Linux. After cloning the code from repository, using `./waf configure` and `./waf build` commands can be executed to install the simulator. Then the sample simulation runs when the command:

```
./waf --run v2x_communication_example
```

is applied. It starts the simulation written in the file `v2x_communication_example.cc` inside the scratch folder. Most of the changes in this study are applied to this file.

In the initial stage, all important parameters including simulation time, CAM packet size, baseline distance, Tx power, P_{rk}, modulation and coding scheme, adjacency mode, sub-channel size, RRI, T_1, T_2, side link bandwidth have to be defined by the user. Then it positions the vehicles randomly inside given limits if there is no mobility model applied outside. If the mobility model is given, the simulator positions nodes for given time instances according to it. For the entire simulation time period, it creates all nodes, networks and the positions(mobility) for each node before starting the simulation.

3.1.2 Implementation of Queues

In [2], all of the properties of CAM packets are not added. It just generates a packet for every chance given for transmission by the SPS algorithm. Therefore, we have created the CAM packet generation behavior as the first implementation of a queue which has generation times and other properties. Before starting the simulation, it creates a CAM packet sequence as an array of C++ objects for the entire simulation time period for each node. Similarly, for the advanced simulations, the DENM queues also have been created with properties like λ, T_D and K of DENM sequences. Both packet queues are merged and given to the transmission function as one queue. For the limitation of final queue length, another dynamic packet queue data structure is introduced. When a chance is given to a UE, it will check the final queue with the current time instance and pick up the correct packet to be transmitted. The queuing delay is calculated as the time interval between packet generation time and the actual transmission time given by the SPS algorithm. Integration of this queuing delay is a key contribution of this research.

3.1.3 Mobility Model (Integration With SUMO)

Most of the simulations done in this study was implemented using static random positions for UEs which were there in the original code, because before integrating the mobility and other infrastructure parameters, we have to make the static simulation working in an acceptable manner with already discovered knowledge. However, in the initial stages of this work, with the help of various online resources, the ability to combine any mobility model into the simulation is established.

First of all, we have to create our mobility model on the vehicular traffic simulator SUMO. There is a good example to build an intersection in [53]. After correcting some typing mistakes in it, the road intersection is built successfully. Using the method described in [54], we are able to get mobility details as a trace file and integrate it with NS-3 simulation.

In the work by Eckermann *et al.* [2] who introduced the simulator modifications for C-V2X, they get an intersection as the worst-case scenario. We expect to compare the results with them as an initial benchmark. The sumo files and NS-3 simulation files which can generate the results mentioned in [2] were not available with the given code repository.

Therefore, the road intersection is created with the knowledge as described above. This creates the `trace.xml` file and it has to be converted to a tcl file which can be fed to NS-3 simulator as the mobility model.

Since we have realized that the simulator in [2] does not have the important features like delay and queuing, this study is oriented to include them. Moreover, most of the radio communication studies were done using the static random positions for the vehicular UEs and we use some of them as benchmarks to compare. Therefore, this mobility model is not implemented for the generation of results mentioned in Chapter 4.

3.1.4 Extracting Information From Logs

There are three main outputs for basic simulation: `simtime`, `tx_data` and `rx_data`. The log `simtime` has a record for each second in simulation time which includes total received packet count, total transmitted packet count and the Packet Reception Ratio (PRR) for cumulative time. The log `tx_data` has a record for each packet transmitted, including data about the transmitter UE's location and transmitting time while the log `tx_data` has a record for each received packet with receiver UE data. For this study, we included some other data related to queuing to the same log files.

The delay is the sum of all delay types as mentioned in Section 2.2. The queuing delay is extracted as the difference between packet generation time recorded in packet information inside the log file `tx_data` and the transmitted time in same file. Transmission delay is extracted using the information in `tx_data`. Packet Reception Ratio (PRR) is directly recorded in the file named `log_simtime`. In this output log, it gives the cumulative average PRR value for each second of simulation. For some simulations, the packet drops outside the queuing were recorded using special log files created for that particular task.

Packet Inter-Reception (PIR) is an impotent parameter mentioned in [2], which calculated using the details of `rx_data` file. It has data transmitted and received time per each UE and per each packet. Therefore, if we need to calculate PIR, we can use these vales. Though this parameter is described in the simulator reference, in this study it is not a highlighted parameter because this study is focused on parameters like CAM packet period as described in the analytical model.

3.2 Simulations

The simulations completed in this study can be divided into 15 main topics. The initial simulations were done to check whether the simulator behavior is in line with well-known theories, and for validation.

List of Simulations

1. The behavior of average PRR and average delay for various CAM packet sizes and node counts. The simulator is implemented without modifications.

2. The behavior of average PRR and average delay for various node counts and three pre-defined Γ values (Assuming T_2 is Γ)

3. The behavior of average PRR and average delay for various RRIs. Repeated for given two bandwidths as in [2].

4. The behavior of average PRR and average delay for various resource re-selection probabilities and two bandwidths.

5. The behavior of average PRR and average delay for various CAM packet periods and three Γ values (Assuming T_2 is Γ)

6. The behavior of average PRR and average delay for various CAM packet periods with delay and three Γ values (T_2 as Γ). This is the first simulation done with added queuing delay.

7. This is the first implementation of basic DENM and variations with CAM packet period. Simulations for the behavior of PRR and average delay against various CAM packet periods and DENM parameters as given in [4].

8. The behavior of average PRR and average delay for three values for Γ (Assuming RRI=T_2=Γ) and various CAM packet periods.

9. With the intention to determine the exact packet drops and delay behavior of simulator, a series of simulations were done using fixed number of nodes, but generation of logs from various points in the code.

10. The behavior of average PRR and average delay with the variation of T_2 and RRI separately.

11. In previous simulations, the queue length is not limited in developed code. Therefore, the number of packet drops due to queuing is not monitored. This simulation is done to observe the behavior of average PRR and average delay with the variation of RRI and CAM packet period under a constant limitation of the queue length.

12. The behavior of average PRR and average delay against the node count for various Γ values. This simulation is further adjusted version using the knowledge from previous simulations.

13. The behavior of average PRR, average delay and physical layer packet drops with various RRIs. In this simulation the independent variable RRI is selected from full range up to 1000ms as mentioned in [26][14].

14. The behavior of average PRR and average delay with various values for P_{rk}.

15. The behavior of average PRR and average delay with various CAM packet period and DENM parameter changes similar to [4].

The simulations 1 to 5 were done as in the repository code without adding queuing delay. In the first simulation, CAM packet sizes and node counts were changed to observe the effect of the simulator on them. Both average delay and PRR did not give a significant response to variation of CAM packet sizes within the standard range (less than 300bytes). However, it has given a response to the node count. The simulations 2, 5, 6 were done assuming T_2 value is the window size (Γ) mentioned in [5]. With the observations, we concluded that the RRI value is the correct parameter in the simulator which is equivalent to Γ. Simulation 3 and 4 are done for the given two bandwidths in [2]. In these simulations, the PRR and delays were checked with various RRI values and various RRP values, respectively.

Average PRR and average delay were observed in simulation 5 by varying the CAM packet period and the T_2 value. First implementation of the queuing delay was done in simulation 6. After simulation 6, the queue was integrated in the simulator as an array. It was observed that a large portion of this delay was added in the initialization time of the simulator. In order to get the outcome closer to a real-world scenario, the first 3 seconds of the simulation were omitted, and sending packets started after that time gap. Following that, the average observed delay was significantly reduced.

First implementation with DENM packets was in simulation 7. The original simulator code only had the CAM packets and basic packet sending implementations. Here, a DENM random generator also had been created according to the known properties of DENM transmissions. The objective was to observe the average delay and the packet reception ratio while changing the properties of DENM transmission with various CAM packet periods.

There were two parameters in the original simulator code named the selection window end time (T_2) and Resource Reservation Interval (RRI). However, according to the reference analytical model [4], the Γ represented both of the above values. Since the response of T_2 as the window size (Γ in the analytical) model was not acceptable in previous simulations, simulation 8 and 10 are done without DENM packets to observe and compare the simulator effect of the T_2 and RRI. Simulation 8 assumed the RRI value and T_2 both are same values and got it as Γ. However, the delay variation was not equivalent with analytical model results. In the 6th simulation, it is observed that in the current simulator structure, the effect of changing the T_2 value on the average delay and the PRR is not significant when the RRI is constant(=100ms). In simulation 10, the effect of RRI is checked by changing RRI when T_2 value is constant at 50ms.

The simulation 9 was done to identify the reason for some of the results to not tally with the analytical model. Here, the aim was to find where the actual packet drops happened when we do not use the queues in simulator code. In that segment, there is a forced packet drop if the distance between Tx and Rx UEs is less than the predefined base line distance, which is set to 150 meters as default. In other simulations, the positions of the vehicular UEs are set to fixed random locations within a 100m x 100m square. Therefore, the distance between any two UEs must not exceed the baseline distance (150m) and the observed packet drop must have happened in the lower layers. For a brief period of time, 50 vehicle UEs were used in multiple parallel simulations to check for those drops, with the functional logs from the simulator classes relating to the MAC, PHY, and RRC layers of the LTE protocol stack. More analysis on the delay implementation on NS-3 is done in Section 4.1.

Although the queuing is added to simulator code after simulation 6, only the delay due to queuing behavior is implemented. Because the queue is not constrained, packet drops that might occur in a real-world scenario owing to queue length limitations are not taken into account. In simulation 11 and the simulations done after it, the queue is limited to predefined constant. The simulation 12 is carried out with some adjustments to the implementation based on the knowledge from prior simulations to observe the effect from the variations with node count and RRI(Γ). Simulation 13 is done to observe the effect of RRI after integration of queuing. In previous simulations, values 20, 50 and 100 (in milliseconds) are assigned as the RRI following the Γ in [4]. However, the RRI can have values 20ms, 50ms, 100ms or any multiple of 100ms [26][14]. Therefore, this simulation is done to observe the effect of all above range possible for RRI.

The simulation 14 is done to observe the effect of Resource Keep Probability (P_{rk}) on the delay and Packet Reception Ratio (PRR). The behavior of DENM messages is checked in simulation 15 with advanced parameter changes after the modifications of the simulator.

Chapter 4

Results and Discussion

4.1 Understanding the Delay of Reference Simulator

In a real-world C-V2X scenario, the delay values are very important as mentioned in Section 2.2. The delay is not considered in the initial simulator study by Eckermann *et al.*[2]. They mentioned that the transmission latency is not taken into account and the propagation delay for the effective distances of 320m is around $1\mu s$. When we consider the base line distance (150m), it is further smaller than 1μs ($150/(3 \times 10^8)$, seconds = 500 nanoseconds). Therefore, the propagation delay is in a negligible range when comparing with other delays. They stated that any further delays caused by processing times are also not included. According to the source-code, we can decide that the queuing delay is also not included with their study.

When executing the given example simulation in [2], the delay value for most of the transmissions were equal to 4928μs. This distribution does not appear to be plausible with a real-world scenario. Therefore, understanding of the current delay values in the simulator was required before continuing with the analysis of delay.

The detailed log for a C-V2X packet transfer is added to this thesis in Appendix A.1. The time is in micro seconds and the value of Transmission Time Interval (TTI) in seconds(0.001s). For that packet transmission, total time difference is 2820928 - 2816000 = 4928 μs . That means it contains 4 times of TTI + 928 μs.

To visualize the effect of TTI, if the defined value in `lte-phy.cc` is increased upto 0.001001 seconds, the detailed log for a packet transfer is as in Appendix A.2. Now the time difference is 2823745 - 2818813 = 4932 μs . That also means it contains 4 times of TTI + 928 μs (1001×4+928=4932). It also has similar components as the previous one. Added component 928 is a constant named `UL_DATA_DURATION` defined in `lte-ue-phy.cc`. Therefore, the delay values in the current log files only depend on the TTI value (which is a predefined constant) in `LTE-PHY`. Clearly, we can get this as the transmission delay component according to the definition in Section 2.2, even though the authors of the simulator mentioned the transmission latency is not considered in their work.

However, when the node count is increased, the delay value was not the same 4928μs for every packet though the average delay is always in the few milliseconds range(more than 4ms). The analysis of these delay values is as shown in Figure 4.1.

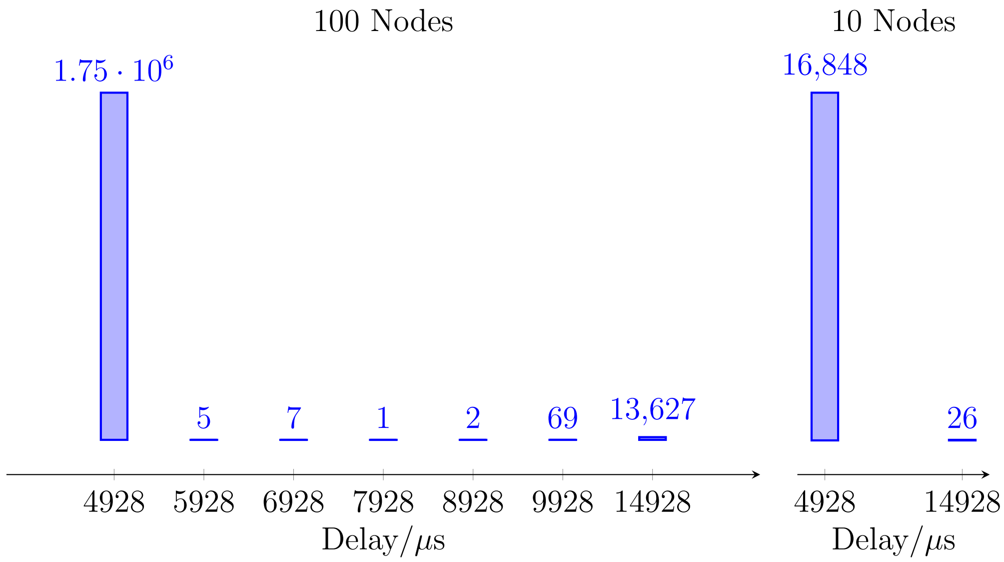

Figure 4.1: Number of packets with discrete delay values
(Implementation of reference simulator of [2])

Since we get this non-realistic delay distribution without changing the size of the packet, this cannot be considered as the transmission delay distribution. Furthermore, when comparing with the queuing delay, the average value added from this distribution was small-scale.

4.2 Behavior With the Node Count

The node count within the selected area is a parameter that significantly impacts communication performance. In this study, we simulate only vehicular nodes (not other nodes like road side unit etc.) with identical conditions except the vehicle's position.

After the new contributions into the code with queuing delay, the simulation 12 was done to observe the effect of the node count. Figure 4.2 and Figure 4.3 shows the response of it when other parameters are set as: CAM packet period=200ms, DENM repetition period(T_D)=100ms, DENM repetitions count(K)=5, DENM distribution parameter(λ)=1. These simulations were done for standard RRI values (20, 50 and 100 milliseconds) with node counts 10, 50, 100, 150, 200 and 250. Figure 4.2 illustrates the Packet Reception Ratio (PRR) variation of our simulations for different Γ values and the similar variation extracted from the benchmark studies [2] and [4] for Γ=100ms. The analytical model [4] presents the collision probability(P_{col}^{v2x}) which has inverse relationship to PRR. Here, the plot is 1-P_{col}^{v2x} for that reference.

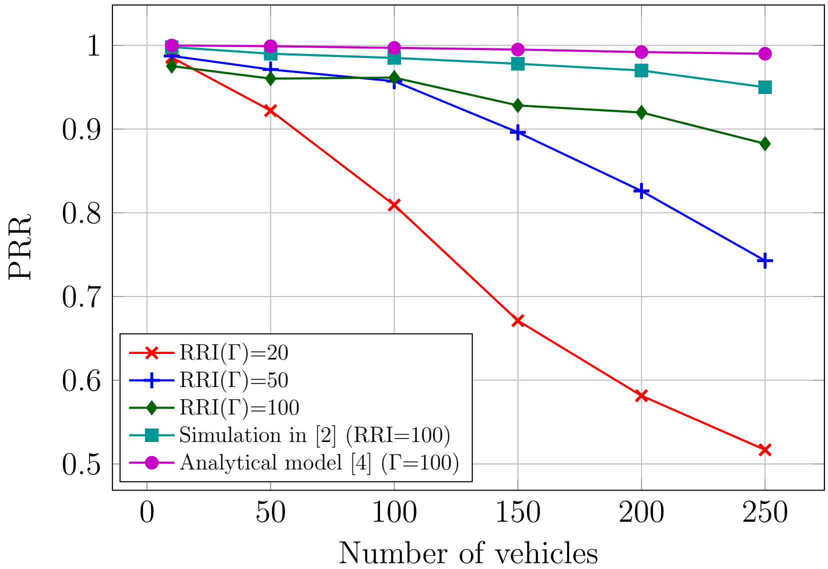

Figure 4.2: PRR with variable node count and RRI(Γ)

For all of these simulations and results, PRR decreases with node count due to the limitation of resources. Our simulation results for all three Γ values give considerably lower PRR than the benchmark studies. Since the physical layer drops are taken into account, we get less PRR than the analytical model. When comparing with the initial simulator, this simulation has a more realistic implementation incorporating DENM generations. The packet drops due to queuing constraints are also considered. Therefore, these PRR values are in an inferior range.

With the increase of Γ, the packet reception is increased, and the effect of increasing the node count is reduced. That is because, for higher Γ, the increase of available resources in the time domain reduces the impact of resource limitation.

The delay variation with node count is illustrated in Figure 4.3. Since the delay is not considered in [2], the delay results for the simulation with original implementation of simulator (Simulation 1) is laid with it to compare. In this, the average delay was 4928μs or slightly more than that for any node count as described in Section 4.1. Because of not having the queuing delay, these values were not in the range given in analytical model. In our simulations with queuing, the delay is almost similar to the analytical model results except some increased fluctuating response for the Γ=100ms. For that exception, the delay was around 200ms and in analytical model, it was 100ms. We can take this difference might be because of the addition of physical layer properties such as random positions with the simulation.

However, both types of results have given no significant response with variation of the

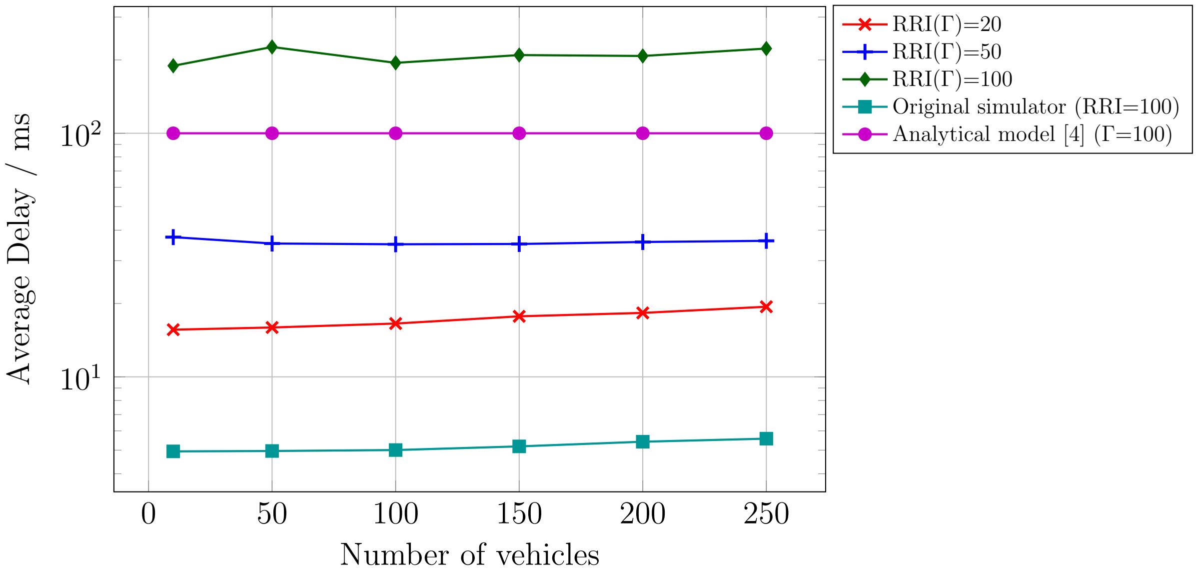

Figure 4.3: Average delay with variable node count and RRI(Γ)

number of nodes. As also mentioned in [4], the scheduling based resource allocation in the standard ensures sufficient radio resources for all nodes even the node count is considerably increased. Therefore the average delay is almost constant with the changes of node count.

4.3 Behavior With Resource Reservation Interval (RRI)

In the analytical model[4], RRI is not considered as a basic independent variable. It presents the response of other parameters when only 20,50 and 100 are assigned for selection window length(Γ) which we get as an equivalent parameter to RRI. Since in this study we extend the simulator in [2] with addition of queuing behavior, the variation of RRI up-to 1000ms is considered as given by them. Therefore, the comparison of RRI is only done with [2].

The plot of PRR and drops illustrated on Figure 4.4 are the results of simulation 13 which we have done to observe the response of RRI with the implementation of queuing and DENM on the simulator. In this simulation, other parameters were configured constant as number of nodes=200, CAM packet period(T_C)=200ms, DENM repetition period(T_D)=100ms, DENM repetitions count(K)=5 and DENM distribution parameter(λ)=1.

In our simulation, the PRR is lower than the PRR in [2] because of the implementation of queuing drops. The overall amount of drops is highly dependent with the number of packets dropped due to queuing limit. When RRI is lower, the queue is not filling like when RRI is higher. That makes high PRR in lower RRIs. However, when we consider only the collisions outside queuing implementation, the drops are happening if higher number of packets are entering to the radio resource space. That drop count will be higher when there are low packet drops in queuing, and high rate of messages which is also illustrated separately in

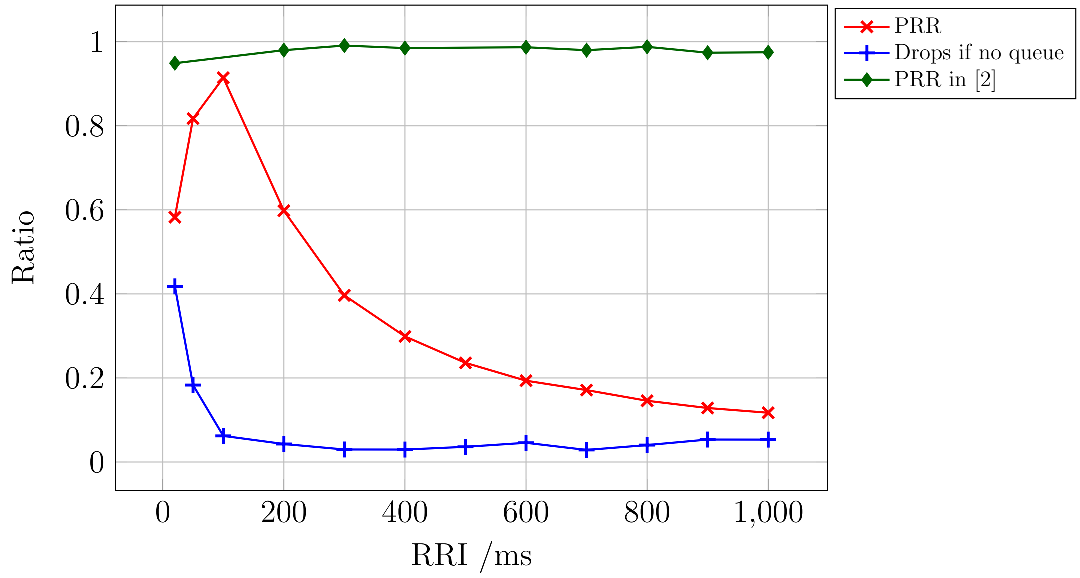

Figure 4.4: PRR and packet drops with RRI(Γ)

Figure 4.4. Therefore, the resultant PRR is not maximum when minimum RRI, due to the effect of that drops outside the queue.

In both of the reference benchmark studies, they do not consider the delay variation with RRI values covering the range of 0 to 1000ms. The behavior of delay in above simulation is illustrated in Figure 4.5. Since this simulation has queuing, if the channel is busy, the packet has to wait in the queue until next Γ interval ends. With the increase of packet generation, the node might have to wait multiple number of Γs until it gets a chance to transmit.

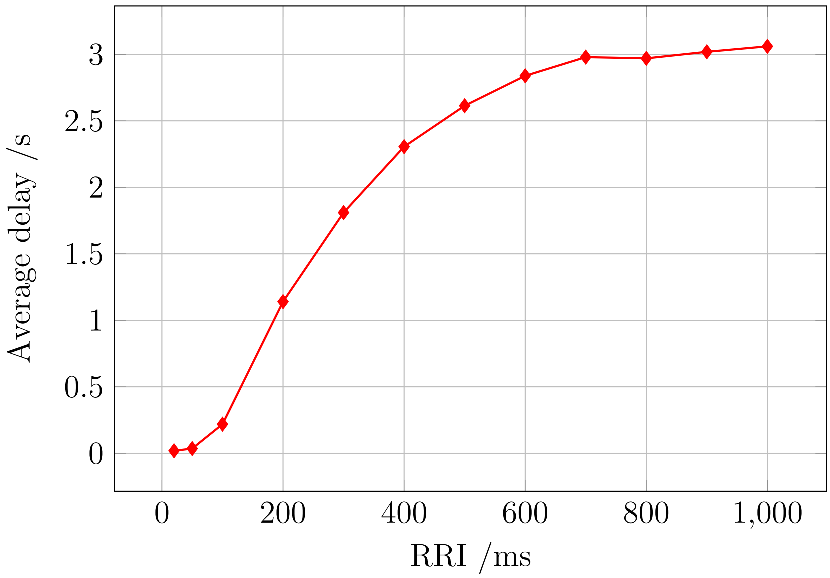

Figure 4.5: Average delay with RRI(Γ)

4.4 Behavior With CAM Packet Period (T_C)

Figure 4.6 shows the PRR captured in Simulation 11 which varied the CAM packet generation rate while maintaining other parameters at constant values: DENM repetition period(T_D) =100ms, DENM repetitions count(K)=5, DENM distribution parameter(λ)=1, number of nodes=100 and T_2=50ms.

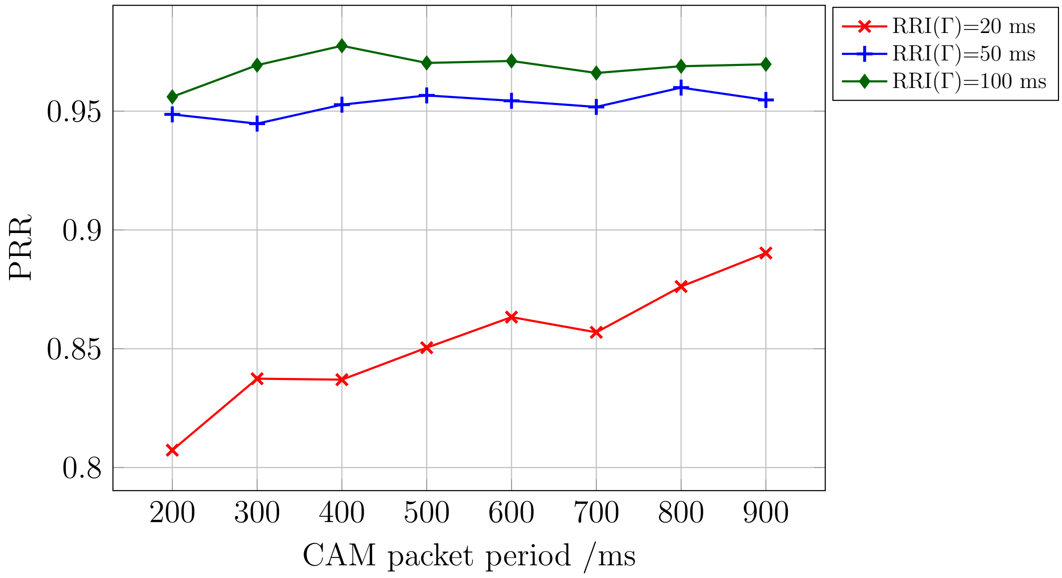

Figure 4.6: PRR with CAM packet rate

Both benchmark studies [2] and [4] do not present the variation of packet reception rate with the packet sending rate or period. As per Figure 4.6, there is no significant variation of the PRR with CAM packet period for RRI values 20ms and 50ms. For 100ms as RRI, the PRR slightly increases with the CAM packet period. When RRI is low, there are higher number of chances to pop packets from the queue. Therefore, the queuing packet drops are not significant for RRI is 50ms or 20ms values. When RRI is 100ms, and low CAM packet periods, the queue has high chance to fill and therefore, low CAM packet periods give low PRRs due to the increasing of packet drops.

In [2], the packet generation rate is not taken into account directly. Therefore, we can use only the analytical model [4] to compare the delay results with CAM packet period. In Figure 4.7, our delay result for above parameters and the variation for Γ=100 in [4] are illustrated.

The delay is significantly higher when RRI is 100ms in both studies. In the analytical model, it goes only up to 180ms, not like simulation result which goes even closer to 1 second delay. This difference might be due to the physical layer effect. According to the analytical model result, there is a minimum value (locally optimal point) of delay when the CAM period is around 300ms. The average delay starts to increase slightly after that point. The

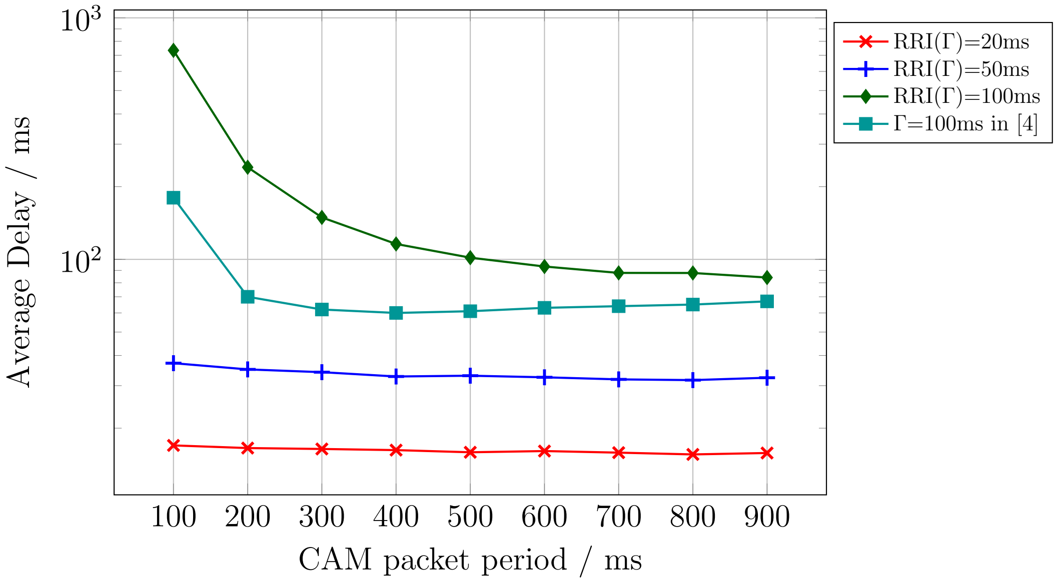

Figure 4.7: Average delay with variable CAM packet period and RRI(Γ)

reason to this locally optimal point is not particularly described. In the simulation results, that phenomenon is not observed.

In the analytical model [4], there are various changes done for the parameters specific to DENM packet generation. After modifying the simulator with all required components for queues and DENM packets, the simulation is done with similar parameters as in [4]. When consider the results in Figure 4.8, the average delay variation is very similar to [4] (Here the graph is illustrated only for the simulation result to improve the readability). However, in the simulation, value of the delay is higher than the expected value of [4]. It is a similar behavior as in previous comparison for Figure 4.7.

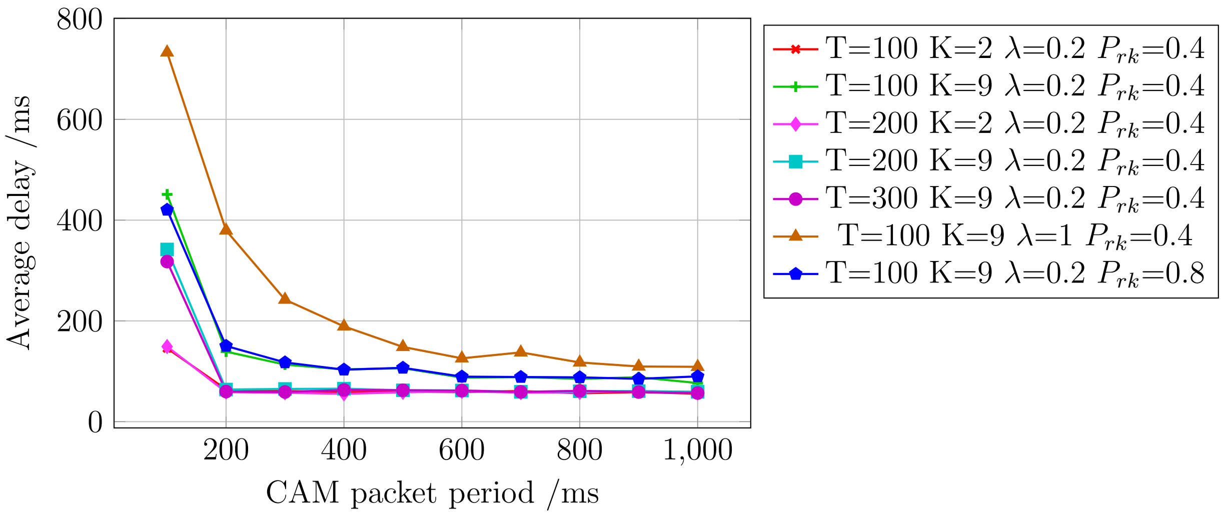

Figure 4.8: Average delay analysis with various DENM properties

4.5 Behavior With Resource Reselection Probability (RRP)

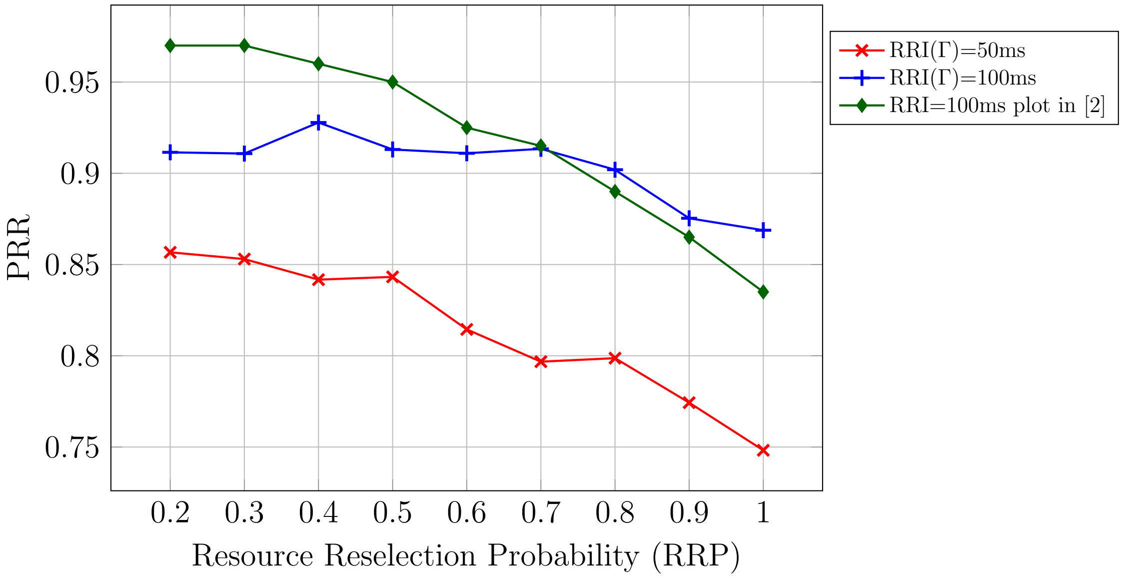

Figure 4.9: Average PRR with RRP

As we mentioned in Section 3.2, the simulation 14 is done to observe the behavior of average PRR and average delay for various values of the P_{rk} for RRI=50ms and 100ms. Other important parameters are taken constant as: number of nodes=200, DENM repetition period(T_D)=100ms, DENM repetitions count(K)=5, DENM distribution parameter(λ)=1 and T_2=50ms. For convenience in comparison here we substitute P_{rk}=1-RRP.

When the RRP increases, UEs select new resources frequently and it makes the communication less predictable as mentioned in [2]. Therefore, SPS does not perform well when the re-selection probability is high. It reduces the reliability of packet reception and the PRR decreases as illustrated in Figure 4.9. For comparison, the static scenario from [2] with 10MHz bandwidth is also included in it.

There is no direct reference to compare the delay. However, in analytical model [4],for Γ = 100 ms, the average delay is slightly higher for P_{rk} is 0.8(RRP=0.2) than 0.4(RRP=0.6) is assigned. For RRI=100ms, average delay is decreased with the re-selection probability. When the RRP is high, the UE gets more chances to encounter the waiting interval(about 50ms) compared to longer RRI(=100ms) [4]. Therefore, the delay decreases for RRI=100 as in Figure 4.10.

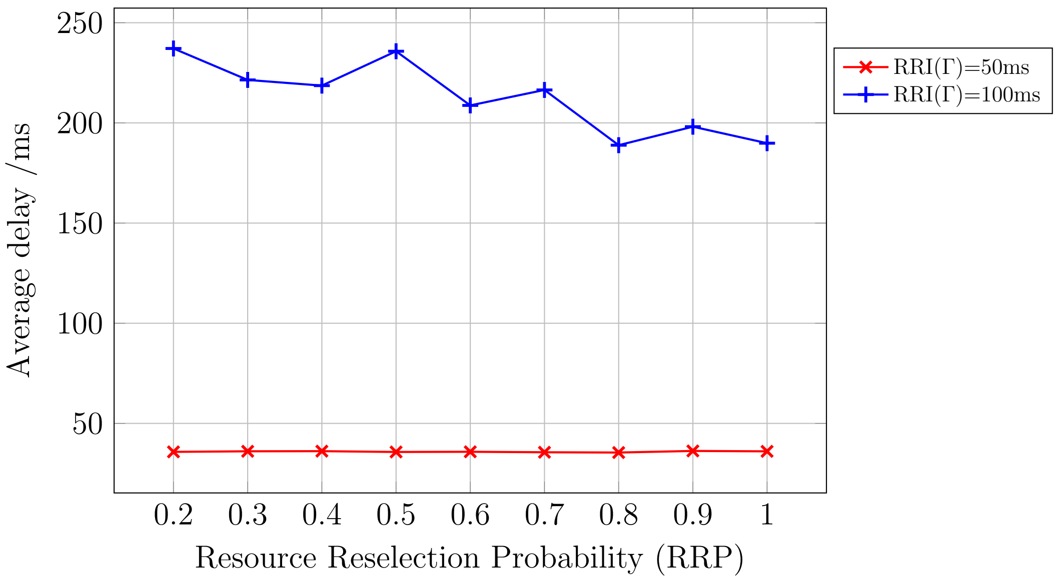

Figure 4.10: Average delay with RRP

Chapter 5

Conclusions

In this simulation-based study, we have done various simulations to observe the effect of key parameters of C-V2X technology. We developed the queuing behavior and the DENM packet generation on simulator library introduced in [2]. After a study on the delay implementation in simulator, a performance analysis is done with comparisons to analytical model [4]. In initial simulations, the results are compared with [2] to confirm that the implementation is correct.

The key outcomes and conclusions of this study are:

- Delay of the simulator introduced in [2] is not a complete implementation which needs to build a realistic simulation in the perspective of delay analysis. We have extended the simulator to fix this gap.
- The packet drops due to queuing limitations are taken into measurements by developing a new queue behavior on NS-3. DENM packet queues are also developed.
- When considering about the response to changes of node count: PRR decreases with node count due to limitation of resources. However, for the small RRI values, PRR is not much affected to the changes of node count. The delay does not give considerable response to node count.
- For the Resource Reservation Interval (RRI), we consider the full range up to 1000ms. The PRR increases with RRI until 100ms and it exponentially decreases for RRI values more than 100ms. The delay increases with RRI although the rate of increasing reduces with node cont.
- CAM packet period: PRR does not give a considerable response to the CAM packet period. However, for 20ms RRI, it makes significant amount of packet drops for low CAM periods and the PRR increases if the CAM packet period is increasing. The

delay decreases with the CAM packet period. Effect of the variation of this parameter is not significant when RRI is less than 100ms. The simulator gives response to CAM packet period very similar to the analytical model when we consider the DENM packet flows with different properties.

- Response to the variation of Resource Reselection Probability (RRP): The PRR decreases with RRP regardless of RRI value. The average delay is almost constant with the RRP for lower RRI values. When RRI is 100ms, the average delay gives small inverse proportional response to RRP

In this study, we have primarily concentrated our efforts on delay implementation in the modified NS-3 simulator of [2]. After a lot of modifications and additions including the queuing delay and drop, the simulation became more realistic as described in analytical model for the delay. And it gives acceptable simulation results also for other parameters like Packet Reception Ratio (PRR). Most of the simulations are done with static random positions for vehicular UEs. As future work, the simulation can be extended to check the response to physical parameters like speed. As an extension to the implementation of queuing, we have done a basic simulation for multi-priority queues following the analytical model in [5]. The simulation-based analysis of it has to be continued.

Appendix A

Detailed Logs to Determine the Delay

A.1 Log Without Modifications

0x55b7aa23ec10 Transmitting V2X PDU at time: 2816000
0x55b7aa2570e0 Now time: 2816000, scheduling next sub frame indication at: 0.001
0x55b7aa23af00 Adjusted Frame no. 283 subframe no. 2
0x55b7aa23d1c0 Now time: 2817000, scheduling next sub frame indication at: 0.001
0x55b7aa23ec10 Adjusted Frame no. 283 subframe no. 2
0x55b7aa23ec10 No SL BSR report to transmit. SL BSR size=1
0x55b7aa2570e0 Now time: 2817000, scheduling next sub frame indication at: 0.001
0x55b7aa23af00 Adjusted Frame no. 283 subframe no. 3
0x55b7aa23d1c0 Now time: 2818000, scheduling next sub frame indication at: 0.001
0x55b7aa23ec10 Adjusted Frame no. 283 subframe no. 3
0x55b7aa2570e0 Now time: 2818000, scheduling next sub frame indication at: 0.001
0x55b7aa23af00 Adjusted Frame no. 283 subframe no. 4
0x55b7aa23d1c0 Now time: 2819000, scheduling next sub frame indication at: 0.001
0x55b7aa23ec10 Adjusted Frame no. 283 subframe no. 4
0x55b7aa2570e0 Now time: 2819000, scheduling next sub frame indication at: 0.001
0x55b7aa23af00 Adjusted Frame no. 283 subframe no. 5
0x55b7aa23d1c0 Now time: 2820000, scheduling next sub frame indication at: 0.001
0x55b7aa2570e0 PSCCH Tx 283/1 rbStart=10 rbLen=2
0x55b7aa2570e0 PSSCH TX 283/1 rbStart=12 rbLen=8
0x55b7aa23ec10 Adjusted Frame no. 283 subframe no. 5
0x55b7aa2570e0 Now time: 2820000, scheduling next sub frame indication at: 0.001
0x55b7aa23d1c0 PSS RNTI 1 cellId 0 has RSRP -108.172 and RBnum 6
0x55b7aa2570e0 PSS RNTI 2 cellId 0 has RSRP -106.907 and RBnum 6
0x55b7aa23af00 Received sidelink packet at time: 2820928

A.2 Log After Small Time Shift

0x558ba1e80c10Transmitting V2X PDU at time: 2818813

0x558ba1e990e0Now time: 2818813, scheduling next sub frame indication at: 0.001001

0x558ba1e7cf00 Adjusted Frame no. 283 subframe no. 2

0x558ba1e7f1c0Now time: 2819814, scheduling next sub frame indication at: 0.001001

0x558ba1e80c10 Adjusted Frame no. 283 subframe no. 2

0x558ba1e80c10 No SL BSR report to transmit. SL BSR size=1

0x558ba1e990e0Now time: 2819814, scheduling next sub frame indication at: 0.001001

0x558ba1e7cf00 Adjusted Frame no. 283 subframe no. 3

0x558ba1e7f1c0Now time: 2820815, scheduling next sub frame indication at: 0.001001

0x558ba1e80c10 Adjusted Frame no. 283 subframe no. 3

0x558ba1e990e0Now time: 2820815, scheduling next sub frame indication at: 0.001001

0x558ba1e7cf00 Adjusted Frame no. 283 subframe no. 4

0x558ba1e7f1c0Now time: 2821816, scheduling next sub frame indication at: 0.001001

0x558ba1e80c10 Adjusted Frame no. 283 subframe no. 4

0x558ba1e990e0Now time: 2821816, scheduling next sub frame indication at: 0.001001

0x558ba1e7cf00 Adjusted Frame no. 283 subframe no. 5

0x558ba1e7f1c0Now time: 2822817, scheduling next sub frame indication at: 0.001001

0x558ba1e990e0PSCCH Tx 283/1 rbStart=10 rbLen=2

0x558ba1e990e0PSSCH TX 283/1 rbStart=12 rbLen=8

0x558ba1e80c10 Adjusted Frame no. 283 subframe no. 5

0x558ba1e990e0Now time: 2822817, scheduling next sub frame indication at: 0.001001

0x558ba1e7f1c0 PSS RNTI 1 cellId 0 has RSRP -108.172 and RBnum 6

0x558ba1e990e0 PSS RNTI 2 cellId 0 has RSRP -106.907 and RBnum 6

0x558ba1e7cf00Received sidelink packet at time: 2823745

Bibliography

[1] 5GAA, "Deployment band configuration for C-V2X at 5.9 GHz in Europe," position paper, 5GAA Automotive Association, 2021.

[2] F. Eckermann, M. Kahlert, and C. Wietfeld, "Performance analysis of c-v2x mode 4 communication introducing an open-source c-v2x simulator," in *2019 IEEE 90th Vehicular Technology Conference (VTC2019-Fall)*, pp. 1–5, 2019.

[3] P. Kyosti, J. Meinila, X. Zhao, C. Schneider, M. N. ć, A. Hong, J. Ylitalo, V.-M. Holappa, M. Alatossava, and T. Rautiainen, "Ist-4-027756 winner ii d1.1.2 v1.1 winner ii channel models," in *2007 IEEE 65th Vehicular Technology Conference - VTC2007-Spring*, IEEE, apr 2007.

[4] G. P. Wijesiri N.B.A., J. Haapola, and T. Samarasinghe, "A discrete-time markov chain based comparison of the mac layer performance of c-v2x mode 4 and ieee 802.11p," *IEEE Transactions on Communications*, vol. 69, no. 4, pp. 2505–2517, 2021.

[5] G. P. Wijesiri N. B. A, J. Haapola, and T. Samarasinghe, "The effect of concurrent multi-priority data streams on the mac layer performance of ieee 802.11p and c-v2x mode 4," *IEEE Transactions on Communications*, vol. 70, no. 1, pp. 592–605, 2022.

[6] 3GPP, "Release 12." `https://www.3gpp.org/specifications/releases/68-release-12`, 2015. Accessed: 2021-09.

[7] 3GPP, "Proximity-based services (ProSe)," Technical Specification (TS) 23.303, 3rd Generation Partnership Project (3GPP), 07 2020. Version 16.0.0.

[8] 3GPP, "Architecture enhancements for 5G System (5GS) to support Vehicle-to-Everything (V2X) services," Technical Specification (TS) 23.287, 3rd Generation Partnership Project (3GPP), 09 2021. Version 17.1.0.

[9] 3GPP, "Evolved Universal Terrestrial Radio Access (E-UTRA);Physical layer procedures," Technical Specification (TS) 36.213, 3rd Generation Partnership Project (3GPP), 10 2021. Version 16.7.1.

[10] 3GPP, "Study on LTE-based V2X services," Technical report (TR) 36.885, 3rd Generation Partnership Project (3GPP), 07 2016. Version 14.0.0.

[11] 3GPP, "Study on LTE support for Vehicle-to-Everything (V2X) services," Technical report (TR) 23.885, 3rd Generation Partnership Project (3GPP), 12 2015. Version 14.0.0.

[12] 3GPP, "Service requirements for V2X services," Technical Specification (TS) 22.185, 3rd Generation Partnership Project (3GPP), 07 2020. Version 16.0.0.

[13] 3GPP, "Enhancement of 3GPP support for V2X scenarios," Technical Specification (TS) 22.186, 3rd Generation Partnership Project (3GPP), 06 2019. Version 16.2.0.

[14] 3GPP, "Evolved Universal Terrestrial Radio Access (E-UTRA); Medium Access Control (MAC) protocol specification," Technical Specification (TS) 36.321, 3rd Generation Partnership Project (3GPP), 09 2021. Version 16.6.0.

[15] 3GPP, "Evolved Universal Terrestrial Radio Access (E-UTRA); Radio Resource Control (RRC); Protocol specification," Technical Specification (TS) 36.331, 3rd Generation Partnership Project (3GPP), 11 2020. Version 16.2.1.

[16] ETSI, "Access layer specification for Intelligent Transport Systems using LTE Vehicle to everything communication in the 5,9 GHz frequency band ," Technical Specification (TS) 103.613, European Telecommunications Standards Institute (ETSI), 11 2018. Version 1.1.1.

[17] ETSI, "Intelligent Transport Systems (ITS);Vehicular Communications;Basic Set of Applications;Part 2: Specification of Cooperative Awareness Basic Service," European Standard (EN) 302 637-2, European Telecommunications Standards Institute (ETSI), 11 2014. Version 1.3.2.

[18] ETSI, "Intelligent Transport Systems (ITS);Vehicular Communications;Basic Set of Applications;Part 3: Specifications of Decentralized Environmental Notification Basic Service," European Standard (EN) 302 637-3, European Telecommunications Standards Institute (ETSI), 11 2014. Version 1.2.2.

[19] 3GPP, "Evolved Universal Terrestrial Radio Access (E-UTRA); User Equipment (UE) radio transmission and reception," Technical Specification (TS) 36.101, 3rd Generation Partnership Project (3GPP), 04 2017. Version 14.3.0.

[20] 3GPP, "Evolved Universal Terrestrial Radio Access (E-UTRA);Physical channels and modulation," Technical Specification (TS) 36.211, 3rd Generation Partnership Project (3GPP), 09 2021. Version 16.7.0.

[21] 3GPP, "Overall description of Radio Access Network (RAN) aspects for Vehicle-to-everything (V2X) based on LTE and NR," Technical Report (TR) 37.985, 3rd Generation Partnership Project (3GPP), 06 2020. Version 16.0.0.

[22] 3GPP, "Vehicle to Vehicle (V2V) services based on LTE sidelink; User Equipment (UE) radio transmission and reception," Technical Report (TR) 36.785, 3rd Generation Partnership Project (3GPP), 10 2016. Version 14.0.0.

[23] 3GPP, "Architecture enhancements for V2X services," Technical Specification (TS) 23.285, 3rd Generation Partnership Project (3GPP), 09 2020. Version 16.4.0.

[24] 3GPP, "Application layer support for Vehicle-to-Everything (V2X) services; Functional architecture and information flows," Technical Specification (TS) 23.286, 3rd Generation Partnership Project (3GPP), 09 2021. Version 17.3.0.

[25] 3GPP, "Study on architecture enhancements for LTE support of V2X services," Technical Report (TR) 23.785, 3rd Generation Partnership Project (3GPP), 09 2016. Version 4.0.0.

[26] R. Molina-Masegosa, J. Gozalvez, and M. Sepulcre, "Comparison of ieee 802.11p and lte-v2x: An evaluation with periodic and aperiodic messages of constant and variable size," *IEEE Access*, vol. 8, pp. 121526–121548, 2020.

[27] "Wireless world initiative new radio ii." `https://cordis.europa.eu/project/id/027756`. Accessed: 2021-10-11.

[28] D. Wang, R. R. Sattiraju, and H. D. Schotten, "Performances of c-v2x communication on highway under varying channel propagation models," in *2018 10th International Conference on Communications, Circuits and Systems (ICCCAS)*, pp. 305–309, 2018.

[29] F. Romeo, C. Campolo, A. Molinaro, and A. O. Berthet, "Denm repetitions to enhance reliability of the autonomous mode in nr v2x sidelink," in *2020 IEEE 91st Vehicular Technology Conference (VTC2020-Spring)*, pp. 1–5, 2020.

[30] H. Seo, K.-D. Lee, S. Yasukawa, Y. Peng, and P. Sartori, "Lte evolution for vehicle-to-everything services," *IEEE Communications Magazine*, vol. 54, no. 6, pp. 22–28, 2016.

[31] R. Rouil, F. J. Cintrón, A. Ben Mosbah, and S. Gamboa, "Implementation and validation of an lte d2d model for ns-3," in *Proceedings of the Workshop on Ns-3*, WNS3 '17, (New York, NY, USA), p. 55–62, Association for Computing Machinery, 2017.

[32] B. Kang, S. Jung, and S. Bahk, "Sensing-based power adaptation for cellular v2x mode 4," in *2018 IEEE International Symposium on Dynamic Spectrum Access Networks (DySPAN)*, pp. 1–4, 2018.

[33] A. Nabil, K. Kaur, C. Dietrich, and V. Marojevic, "Performance analysis of sensing-based semi-persistent scheduling in c-v2x networks," in *2018 IEEE 88th Vehicular Technology Conference (VTC-Fall)*, pp. 1–5, 2018.

[34] R. Molina-Masegosa and J. Gozalvez, "System level evaluation of lte-v2v mode 4 communications and its distributed scheduling," in *2017 IEEE 85th Vehicular Technology Conference (VTC Spring)*, pp. 1–5, IEEE, jun 2017.

[35] R. Molina-Masegosa, J. Gozalvez, and M. Sepulcre, "Configuration of the c-v2x mode 4 sidelink pc5 interface for vehicular communication," in *2018 14th International Conference on Mobile Ad-Hoc and Sensor Networks (MSN)*, pp. 43–48, 2018.

[36] Y. Jeon, S. Kuk, and H. Kim, "Reducing message collisions in sensing-based semi-persistent scheduling (sps) by using reselection lookaheads in cellular v2x," *Sensors*, vol. 18, no. 12, 2018.

[37] D. Wang, R. R. Sattiraju, A. Weinand, and H. D. Schotten, "System-level simulator of lte sidelink c-v2x communication for 5g," in *Mobile Communication - Technologies and Applications; 24. ITG-Symposium*, pp. 1–5, 2019.

[38] B. Toghi, M. Saifuddin, H. N. Mahjoub, M. O. Mughal, Y. P. Fallah, J. Rao, and S. Das, "Multiple access in cellular v2x: Performance analysis in highly congested vehicular networks," in *2018 IEEE Vehicular Networking Conference (VNC)*, pp. 1–8, 2018.

[39] W. Anwar, N. Franchi, and G. Fettweis, "Physical layer evaluation of v2x communications technologies: 5g nr-v2x, lte-v2x, ieee 802.11bd, and ieee 802.11p," in *2019 IEEE 90th Vehicular Technology Conference (VTC2019-Fall)*, pp. 1–7, 2019.

[40] V. Mannoni, V. Berg, S. Sesia, and E. Perraud, "A comparison of the v2x communication systems: Its-g5 and c-v2x," in *2019 IEEE 89th Vehicular Technology Conference (VTC2019-Spring)*, pp. 1–5, 2019.

[41] J. P. Jeyaraj and M. Haenggi, "Reliability analysis of v2v communications on orthogonal street systems," in *GLOBECOM 2017 - 2017 IEEE Global Communications Conference*, pp. 1–6, 2017.

[42] Y. Fan, L. Liu, S. Dong, L. Zhuang, J. Qiu, C. Cai, and M. Song, "Network performance test and analysis of lte-v2x in industrial park scenario," *Wireless Communications and Mobile Computing*, vol. 2020, pp. 1–12, 12 2020.

[43] T. Hirai and T. Murase, "Noma concept for pc5-based cellular-v2x mode 4 in crash warning system," in *2019 IEEE 90th Vehicular Technology Conference (VTC2019-Fall)*, pp. 1–6, 2019.

[44] T. V. Nguyen, P. Shailesh, B. Sudhir, G. Kapil, L. Jiang, Z. Wu, D. Malladi, and J. Li, "A comparison of cellular vehicle-to-everything and dedicated short range communication," in *2017 IEEE Vehicular Networking Conference (VNC)*, pp. 101–108, 2017.

[45] V. Vukadinovic, K. Bakowski, P. Marsch, I. D. Garcia, H. Xu, M. Sybis, P. Sroka, K. Wesolowski, D. Lister, and I. Thibault, "3gpp c-v2x and ieee 802.11p for vehicle-to-vehicle communications in highway platooning scenarios," *Ad Hoc Networks*, vol. 74, pp. 17–29, 2018.

[46] J. Thota, N. F. Abdullah, A. Doufexi, and S. Armour, "Performance of car to car safety broadcast using cellular v2v and ieee 802.11p," in *2018 IEEE 87th Vehicular Technology Conference (VTC Spring)*, pp. 1–5, 2018.

[47] G. Cecchini, A. Bazzi, B. M. Masini, and A. Zanella, "Performance comparison between ieee 802.11p and lte-v2v in-coverage and out-of-coverage for cooperative awareness," in *2017 IEEE Vehicular Networking Conference (VNC)*, pp. 109–114, 2017.

[48] G. Naik, B. Choudhury, and J.-M. Park, "Ieee 802.11bd amp; 5g nr v2x: Evolution of radio access technologies for v2x communications," *IEEE Access*, vol. 7, pp. 70169–70184, 2019.

[49] J. Santa, F. Pereñíguez, A. Moragón, and A. F. Skarmeta, "Vehicle-to-infrastructure messaging proposal based on cam/denm specifications," in *2013 IFIP Wireless Days (WD)*, pp. 1–7, 2013.

[50] D. Martín-Sacristán, S. Roger, D. Garcia-Roger, J. F. Monserrat, A. Kousaridas, P. Spapis, S. Ayaz, and C. Zhou, "Evaluation of lte-advanced connectivity options for the provisioning of v2x services," in *2018 IEEE Wireless Communications and Networking Conference (WCNC)*, pp. 1–6, 2018.

[51] X. He, J. Lv, J. Zhao, X. Hou, and T. Luo, "Design and analysis of a short-term sensing-based resource selection scheme for c-v2x networks," *IEEE Internet of Things Journal*, vol. 7, no. 11, pp. 11209–11222, 2020.

[52] "ns-3 network simulator." `https://www.nsnam.org/`, 2021. Accessed: 2021-01.

[53] "Controlled intersection in sumo." `https://sites.google.com/site/codedwise/sumo-tutorials/controlled-intersection-in-sumo`, 2021. Accessed: 2021-01.

[54] "Tracing vehicular mobility in ns-3." https://www.opensourceforu.com/2017/11/tracing-vehicular-mobility-ns-3/, 2021. Accessed: 2021-01.